

1 ARTICLE TEMPLATE

2 **Ocean Heat Content Variability in the Bay of Bengal: A CMIP6 Model**  
3 **Analysis with implications on Indian Ocean Dipole**

4 A. B. Asok<sup>a</sup>, A. P. Joshi<sup>a</sup>, and H. V. Warrior<sup>a\*</sup>

5 <sup>a</sup>Department of Ocean Engineering and Naval Architecture, IIT Kharagpur, Kharagpur- 721302, West  
6 Bengal, India

7 **ARTICLE HISTORY**

8 Compiled October 10, 2023

9 **ABSTRACT**

10 This study evaluates the performance of CMIP6 models in capturing Ocean Heat Content  
11 (OHC) variations in the Bay of Bengal. The Seawater Potential Temperature (Thetao) of the  
12 six best-performing models up to a depth of 500 m from the sea surface is chosen for the study  
13 on a 1° x 1° horizontal resolution and monthly temporal scale and compared with RAMA buoy  
14 and North Indian Ocean Atlas( NIOA) data. Performance indices such as RMSE, average error,  
15 AAE, and Willmott score are used. The GISS-E2-1-G model exhibits better performance with  
16 lower Root Mean Square Error (RMSE) and Absolute Average Error (AAE) values, while the  
17 IPSL-CM6A-LR model performs poorly. Monthly climatology variations show an increase in  
18 temperature and OHC during the summer season. Annual trends in OHC reveal negative trends  
19 for some models, indicating a net loss of heat, while others show positive trends, indicating  
20 heat accumulation. Comparison with RAMA Buoy data consistently shows lower heat con-  
21 tent compared to the models, indicating overestimation. The study emphasizes the importance  
22 of incorporating observational data to improve accuracy. The findings highlight variations in  
23 model performance and the need for understanding uncertainties and biases in climate models  
24 for reliable projections. Additionally, the study suggests that the interaction between the North  
25 and South Bay of Bengal can have implications for the Indian Ocean Dipole phenomenon,  
26 influencing temperature gradients and hence the OHC.

27 **KEYWORDS**

28 CMIP6; Climate prediction; Bay of Bengal; OHC

---

CONTACT H. V. Warrior. Email: warrior@naval.iitkgp.ernet.in

## 1. Introduction

The Earth's climate is undergoing rapid changes driven by various factors, with human activities such as the burning of fossil fuels, industrialization, and deforestation playing a significant role. A crucial indicator of climate change is the Earth's energy imbalance, which refers to the disparity between the amount of heat energy entering the Earth's atmosphere from the sun and the amount radiated back into space.<sup>1</sup> Disturbances in this energy balance can result in either cooling or warming of the Earth's surface, leading to alterations in weather patterns, sea-level rise, and other consequential effects. Monitoring changes in Ocean Heat Content (OHC) and the Earth's energy imbalance is vital for comprehending and predicting the impacts of climate change.<sup>2</sup>

Climate modeling plays a central role in climate change studies and has become an expanding field within climate research. The advancements in general circulation models now allow for the investigation of historical climate variations and future climate projections. The international climate modeling community collaborates every few years to employ the latest versions of their climate models in a coordinated set of simulations.<sup>3</sup> Through this model intercomparison, the climate science community can assess the performance of models in comparison to older versions and newer models. Moreover, the ensemble of model results supports a range of climate change impact and adaptation studies, as well as public outreach and education. Utilizing an ensemble of models within a standard experimental framework enables scientists to compute ensemble statistics, enhancing the accuracy of projections and allowing for quantification of the associated confidence or uncertainty. This successful global collaboration is known as the Coupled Model Intercomparison Project (CMIP).<sup>4</sup>

The latest phase of the Coupled Model Intercomparison Project, CMIP6, under the World Climate Research Programme (WCRP), presents an opportunity to examine several simulated global Ocean General Circulation Models (OGCMs).<sup>5</sup> The objective of this research is to develop a suite of models that can more accurately replicate the oceans and climate. The CMIP6 models, incorporating both natural and anthropogenic forcing, provide historical simulations from 1850 to 2014, along with prospective scenarios of tiers 1 and 2<sup>6</sup>. The tier 1 socioeconomic scenarios (SSPs) include revised versions of the CMIP5 Representative Concentration Pathway (RCPs), such as SSP1-2.6, SSP2-4.5, SSP3-7.0, and SSP5-8.5.

The Indian Ocean, the world's third-largest ocean, plays a crucial role in the Earth's climate system. Over the past few decades, the Indian Ocean, particularly the Bay of Bengal (BoB), has been experiencing accelerated warming compared to other oceans, leading to sig-

nificant impacts on regional climate, coastal communities, and marine ecosystems.<sup>7</sup> The Bay of Bengal, located in the northeastern part of the Indian Ocean, covers an area of approximately 2.17 million square kilometers and is bordered by several countries, including India, Bangladesh, Myanmar, Thailand, and Sri Lanka. Characterized by warm water, the Bay of Bengal is influenced by the southwest and northeast monsoons,<sup>8</sup> which bring heavy rainfall to the surrounding regions. It is also prone to tropical cyclones, primarily occurring from October to November.<sup>9</sup> The bay is home to diverse marine life and natural resources, making it an important fishing ground that supports the livelihoods of coastal communities. The Bay of Bengal exhibits significant temperature variations throughout the year. During the winter season, cooler and less saline water from the northern region flows southward, forming a surface layer. In contrast, warm and saline waters from the equatorial region, influenced by the southwest monsoon, create a warmer layer near the surface during the summer season.<sup>10</sup> Additionally, the Bay receives freshwater inputs from several rivers, including the Ganges, Brahmaputra, and Irrawaddy.<sup>11</sup> These rivers carry a significant amount of freshwater during the monsoon and post monsoon season,<sup>12</sup> creating a less saline surface layer and potentially leading to stratification within the water column. Such stratification has important implications for the distribution of marine organisms, nutrient availability, and flow patterns in the bay.

Ocean Heat Content (OHC) is a significant parameter in Oceanography that has been extensively studied through modeling. Several studies have been conducted at regional and global scales to estimate changes in Ocean Heat Content (OHC) on inter-seasonal, inter-annual, and inter-decadal time scales. Measuring and monitoring OHC is important because it provides valuable information about the energy balance of the Earth.<sup>13</sup> Changes in OHC can indicate the presence of climate variations and trends, as well as the impact of climate change.<sup>14</sup> It is an essential component in assessing the overall energy imbalance of the planet.<sup>15</sup> In this study, we focus on the Bay of Bengal and examine Seawater Potential Temperature (thetao) data and associated OHC up to a depth of 500 m from the sea surface. The data is obtained from six CMIP6 models and is compared with NIOA data and RAMA Buoy data located at (15°N 90°E). This analysis aims to provide a comprehensive understanding of the variation in Ocean Heat Content within the Bay of Bengal over different seasons and years. The study region encompasses latitudes ranging from 0°N and 24°N latitudes and 78°E and 100°E longitudes. Due to the unique air-sea interaction and dynamics in this region, investigating Ocean Heat Content in the Bay of Bengal contributes to a deeper understanding of climate

95 processes in the area.

## 96 **2. Data**

### 97 **2.1. Study Area**

98 The Bay of Bengal (BoB) region exhibits a high degree of stratification, primarily attributed  
99 to the abundant freshwater input and limited vertical mixing. This unique combination has  
100 led to the formation of a dense barrier layer, resulting in elevated sea surface temperatures  
101 (SST) throughout the basin. To study the BoB region, the investigation focuses on the area  
102 between latitudes 0° N and 24° N, and longitudes 78° E and 100° E. The bathymetric data  
103 for the region is derived from the General Bathymetric Chart of the Oceans (GEBCO 08).  
104 The analysis encompasses the western coast and the northern estuary, which exhibit varying  
105 depths, typically around 150 meters. However, the presence of the Swatch of No Ground  
106 (SoNG), a submarine canyon reaching a depth of 1200 meters, adds complexity to the region.  
107 The remainder of the study area consists of the deep open ocean.

108 In the BoB, gathering comprehensive data on physical and biological oceanographic pa-  
109 rameters has been challenging due to limited field expeditions. Consequently, modeling ap-  
110 proaches are employed to compensate for the scarcity of data. Model efficacy becomes cru-  
111 cial for replicating the physical and biogeochemical dynamics accurately. However, computa-  
112 tional limitations often require coarser resolutions in these models. To enhance the predictabil-  
113 ity of these models, modern parameterization schemes for heat content in the ocean, which  
114 heavily influence ocean dynamics, are employed.

### 115 **2.2. CMIP6 models**

116 The Coupled Model Inter Comparison Project phase 6 ([https://esgf-node.llnl.gov/p](https://esgf-node.llnl.gov/projects/cmip6/)  
117 [rojects/cmip6/](https://esgf-node.llnl.gov/projects/cmip6/)) offered data sets from CMIP6 multi-model archive which were utilized  
118 in the analysis. Based on best-performing temperature models (16), (17), (18) in the Bay of  
119 Bengal, six CMIP6 models are selected for the study. Table 1 shows the models employed in  
120 the research. In this study, the historical simulations of six coupled models, a single ensemble  
121 (r1i1p1f1), and four Tier 1 CMIP6 socio-economical projection scenarios (ssp126, ssp245,  
122 ssp370, and ssp585) are used to examine the efficiency in simulating the seasonal and annual  
123 variability of ocean heat content over the Bay of Bengal region.

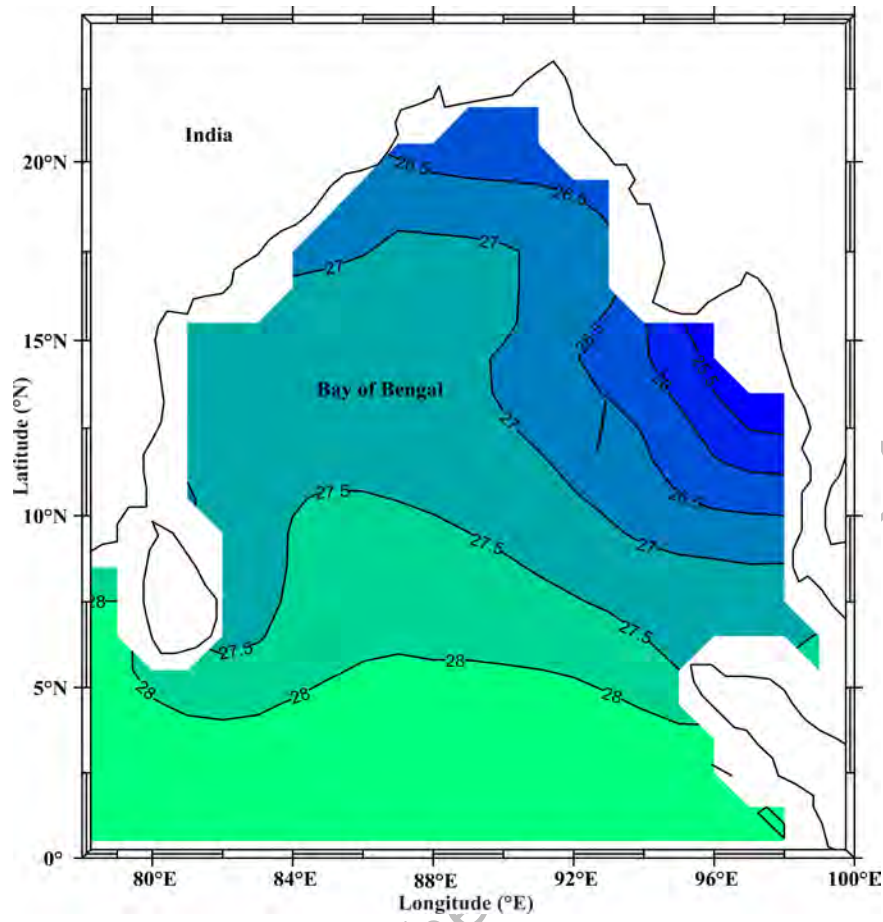


Figure 1.: Study Area

Table 1.: Selected CMIP6 Models giving OHC

CMIP6 Models	Variant Label	Frequency	Experiment ID	Res	Reference Journals
CanESM5	rlilp1fl	Monthly	Historical	100 km	(16; 17)
GISS-E2-1-G	rlilp1fl	Monthly	Historical	250 km	(18)
IPSL-CM6A-LR	rlilp1fl	Monthly	Historical	100 km	(16; 17)
MPI-ESM-1-2HAM	rlilp1fl	Monthly	Historical	100 km	(17)
MPI-ESM1-2-HR	rlilp1fl	Monthly	Historical	50 km	(17)

MPI-ESM1- 2-LR	r11p1f1	Monthly	Historical	50 km	(17; 18)
-------------------	---------	---------	------------	-------	----------

### 124 **2.3. NIOA Data**

125 For the Indian Ocean region, the North Indian Ocean Atlas (NIOA) serves as the climato-  
 126 logical atlas. NIOA aims to improve upon the World Ocean Atlas (WOA) by incorporating  
 127 additional data from Indian sources, explicitly focusing on the Indian Exclusive Economic  
 128 Zone (EEZ). By including this additional data, the NIOA provides a more comprehensive  
 129 and accurate representation of temperature and salinity in the Indian Ocean, particularly in  
 130 the Bay of Bengal. One significant improvement of the NIOA compared to the WOA is the  
 131 elimination of patchiness seen in the Bay of Bengal, which was an artifact of the sparsity  
 132 of data in the WOA. This data collection serves as the basis for the current study's valida-  
 133 tion of the Seawater potential temperature and other physical processes. The info comes from  
 134 <https://publication-data.nio.org/s/q7g6t84j4YTKiGz>. The monthly average  
 135 climatology temperature up to the depth of 500 m is used from January 1950 to December  
 136 2014.

### 137 **2.4. RAMA BUOY Data**

138 The Research Moored Array for African-Asian-Australian Monsoon Analysis and Prediction  
 139 (RAMA) is used in this study for the comparison of different CMIP6 models to identify the  
 140 better performance of the models in the Bay of Bengal. The RAMA buoy is part of an in-  
 141 ternational research project aimed at improving the understanding and prediction of the In-  
 142 dian Ocean and its monsoon system. The RAMA buoy array consists of a series of moored  
 143 buoys equipped with various instruments to measure meteorological and oceanographic pa-  
 144 rameters. These buoys are strategically located throughout the Indian Ocean, including the  
 145 Bay of Bengal. The observations from the buoys provide valuable data on sea surface temper-  
 146 ature, air temperature, wind speed and direction, humidity, atmospheric pressure, and other  
 147 relevant variables. The data collected from the RAMA buoys are crucial for studying the  
 148 Indian Ocean's climate variability, the Indian Ocean Dipole (IOD), El Nino-Southern Oscil-  
 149 lation (ENSO), and the monsoon system. The Buoy is located at ( $15^{\circ}N$   $90^{\circ}$ ) and is used for  
 150 the validation from January 2007 to December 2014, the depth wise (500m) monthly averaged

151 temperature is permuted to climatology data.

### 152 3. Methodology

153 The resolutions of CMIP6 models are changed to a standard of 1°x 1° and converted into  
154 monthly climatology data for reliable comparison. The six best-performing CMIP6 models  
155 are taken into account and listed in Table1. The CMIP6 model data are compared with NIOA  
156 data from 1950-2014. The study uses various statistical techniques to assess the effectiveness  
157 of the CMIP6 model in stimulating Ocean Heat Content. Grids with where observation values  
158 were available are selected for the model assessment to prevent statistical error.

159 OHC is typically measured as the amount of heat energy per unit area or volume of the  
160 ocean. Scientists use a combination of observational data and computer models to estimate and  
161 analyze OHC on different time scales, ranging from seasonal to decadal and longer. Advanced  
162 technologies such as Argo floats, satellite remote sensing, and historical data from research  
163 vessels are used to gather information about temperature profiles and thermal properties of  
164 the ocean. The Ocean Heat Content is calculated by using the equation

$$OHC = \int_0^z \rho \cdot Cp \cdot \theta \cdot dz \quad (1)$$

165 where  $\rho$  is the density of seawater taken as 1026 Kg/m<sup>3</sup>,  $Cp$  is the specific heat capacity of  
166 the seawater taken as 4000 Kg/J,  $\theta$  is the seawater potential temperature  $z$  is the water depth  
167 500 m of the water column from the sea surface.

#### 168 3.1. The Measures of Efficiency

169 For the analysis of the best-performing model in the Bay of Bengal region, different Perfor-  
170 mance matrices are used for statistical analysis in the study.

##### 171 3.1.1. Willmott skill score

172 Compared to previously reported approaches, the Willmott index (WI) is a more sophisticated  
173 way to assess the performance of a model (19). The degree to which the measured variations  
174 can be accounted for by the model can be expressed using Willmott's index (WI), which is  
175 sensitive to variations between the measured and modeled value and has a range of 0 to 1.  
176 A Willmott Index of 0 denotes either a lack of agreement between the model and observa-

177 tion or insufficient variety in the observations to fully test the model, while 1 denotes perfect  
178 agreement between the model and observation.

$$WI = 1 - \frac{\sum_{i=1}^n (m_i - o_i)^2}{|m_i - \bar{o}| + |o_i - \bar{o}|^2} \quad (2)$$

179

### 180 3.1.2. Correlation Coefficient ( $r$ )

181 The correlation coefficient ( $r$ ) provides a measure of the dissimilarity and association between  
182 the model and observed variables. In the present research, the correlation coefficient is em-  
183 ployed to assess the temporal variability of Ocean Heat Content. Its values range from -1 to  
184 +1, where a positive value signifies agreement between the modeled and predicted values,  
185 while a negative value indicates a lack of agreement.

$$r = \frac{\sum_{i=1}^n (o_i - \bar{o})(m_i - \bar{m})}{\sqrt{\sum_{n=1}^N (o_i - \bar{o})^2 \sum_{i=1}^n (m_i - \bar{m})^2}} \quad (3)$$

186

### 187 3.2. Errors

188 The evaluation of the disparities between the model and expected values involves several  
189 error metrics, including Root Mean Square Error (RMSE), Average Absolute Error (AAE),  
190 and Average Error (AE). These measures provide insights into the magnitude and direction of  
191 the errors between the model predictions and the anticipated values.

$$RMSE = \sqrt{\frac{\sum_{n=1}^N (m_i - o_i)^2}{N}} \quad (4)$$

192 This suggests that a number close to zero denotes a good fit between the model and the  
193 observed values.

$$AE = \bar{m} - \bar{o} \quad (5)$$



194 Since a few of the errors may cancel due to sign difference, AE occasionally does not present  
195 a complete picture.

$$AAE = \frac{\sum_{n=1}^N |m_i - o_i|}{N} \quad (6)$$

196 AAE and RMSE are used to address this flaw and eliminate the mismatch.

$$STD = \sqrt{\frac{\sum_{n=1}^N (m_i - o_i)^2}{N - 1}} \quad (7)$$

197

198 where STD is the standard deviation, N is the number of observations,  $o_i$  is the  $i^{\text{th}}$  obser-  
199 vation value,  $m_i$  is the  $i^{\text{th}}$  model simulated value,  $\bar{o}$  is the Mean of the observations, and  $\bar{m}$  is  
200 the Mean of the model simulated values.

201 To calculate the confidence interval for a normal distribution, we need;

- 202 • The sample mean
- 203 • The sample standard deviation
- 204 • The sample size
- 205 • The desired confidence level

206 The confidence level is the percentage of the time that the confidence interval is expected to  
207 contain the true dataset mean. In our calculation, we use a confidence level of 95%.

208 Once we have this information, we can use the following formula to calculate the confi-  
209 dence interval:

210

Confidence interval = sample mean  $\pm$  (critical value of the z-distribution) \* (standard error  
211 of the mean). (8)

212 The critical value of the z-distribution can be found in a z-table and for 95% confidence  
213 interval and is taken as 1.96. Then we have calculated the confidence interval for all the 6  
214 models (Table 3).

Table 2.: Validation indices of various CMIP6 models

Models	Sync Indicator	Error Indicator			
	r	RMSE ( $\times 10^{10}$ )	AE ( $\times 10^{10}$ )	AAE ( $\times 10^9$ )	STD ( $\times 10^{10}$ )
CanESM5	0.87	1.5	-8.39	8.75	2.02
GISS-E2-1-G	0.91	1.36	-4.58	6.13	2.38
IPSL-CM6A-LR	0.89	1.68	-0.95	9.84	1.88
MPI-ESM-1-2HAM	0.88	1.61	-7.96	8.82	2.06
MPI-ESM1-2-HR	0.92	1.44	-7.02	8.00	2.09
MPI-ESM1-2-LR	0.88	1.60	-7.92	8.77	2.06

The standard error of the mean is calculated as follows:

$$\text{Standard error of the mean} = \text{sample standard deviation} / \sqrt{(\text{sample size})} \quad (9)$$

#### 4. Results and Discussion

To assess the model's agreement with the NIOA (National Institute of Oceanography and Applied Geophysics) data, five performance indices and Willmott skill scores are utilized. The CMIP6 (Coupled Model Intercomparison Project Phase 6) models are standardized to a resolution of  $1^\circ \times 1^\circ$  to ensure a valid comparison with the NIOA data. These models are evaluated based on the calculated performance indices and skill scores. The statistical matrix, including Root Mean Square Error (RMSE), Average Error (AE), Average Excess Error (AEE), and correlation, as employed in previous studies.<sup>20,16</sup> The skill score is then used to rank the considered CMIP6 models Fig. 1. Table 2 shows the performance statistics for all CMIP6 models discussed below. The confidence interval for the various models are given in Table3

##### 4.1. Identification of the model

The values of performance indices for the selected 6 CMIP6 models are shown in Table2. The RMSE is observed to be the minimum for the GISS-E2-1-G ( $1.36 \times 10^{10}$ ) and maximum for IPSL-CM6A-LR ( $1.68 \times 10^{10}$ ). The average error is negative for all of the models indicating the predicted values are lower than the actual values. The absolute average error (AAE) is

Table 3.: confidence interval for the various models

Models	Margin of error	Confidence interval)(*e+10)
CanESM5	3.11e+07	4.84-4.85
GISS-E2-1-G	3.72e+07	4.84-4.85
IPSL-CM6A-LR	2.38e+07	3.85-3.86
MPI-ESM-1-2HAM	4.06e+07	4.21-4.22
MPI-ESM1-2-HR	3.35e+07	4.25-4.26
MPI-ESM1-2-LR	3.21e+07	4.22-4.33

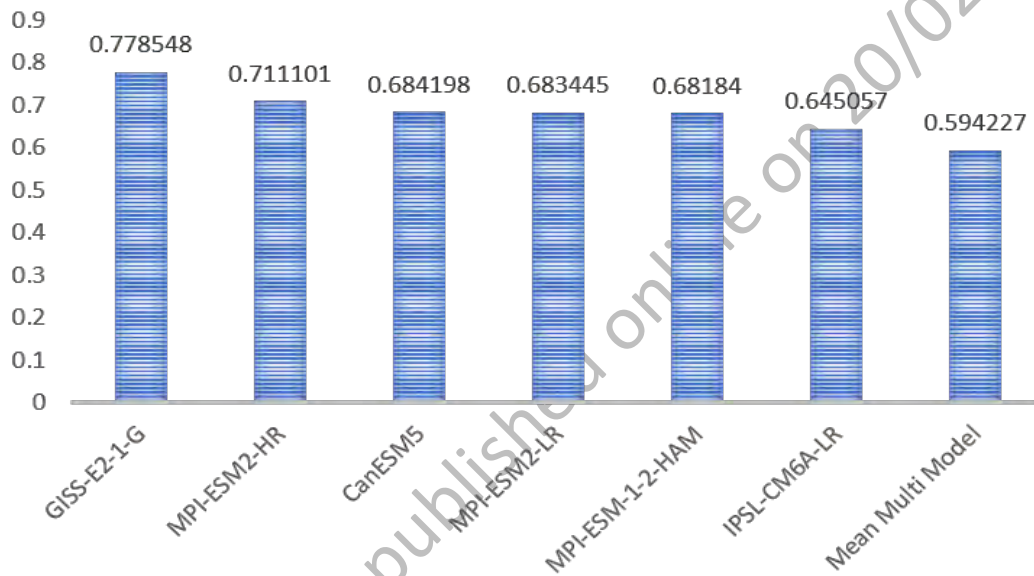


Figure 2.: Skill score for CMIP6 models compared with the NIOA data.

233 maximum for IPSL-CM6A-LR ( $9.84 \times 10^9$ ) which suggests that the model is not performing  
 234 well and minimum for GISS-E2-1-G ( $6.13 \times 10^9$ ). The Willmott score analysis reveals that  
 235 the IPSL-CM6A-LR model exhibits poor performance (score of 0.64) compared to all other  
 236 models, while the GISS-E2-1-G model demonstrates relatively better performance (score of  
 237 0.77) in the Bay of Bengal region. In general, all the models exhibit strong correlations in  
 238 the vicinity of the bay and the southern part of the Bay of Bengal. However, a distinct spa-  
 239 tial pattern emerges, indicating zero correlation and p-values greater than 0.5 in the central  
 240 region (see Figure 4). Bias, on the other hand, signifies the systematic deviation or disparity  
 241 between two datasets or models. A positive bias implies that one dataset or model consistently

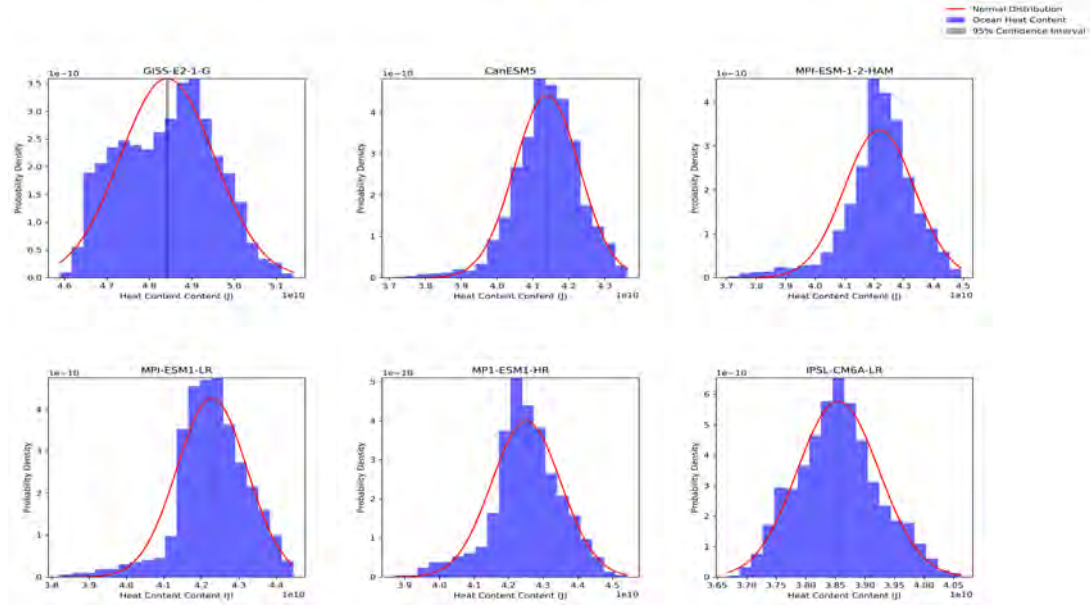


Figure 3.: Normal distribution for CMIP6 models OHC data.

overestimates the other, whereas a negative bias suggests consistent underestimation. In this analysis, all the models demonstrate positive bias, indicating that they tend to overestimate the reference datasets.

Furthermore, specific models exhibit varying levels of bias in different regions of the Bay of Bengal (see Figure 3). The models MPI-ESM1-2-LR, MPI-ESM1-2HAM, MPI-ESM1-2-HR, and CanESM5 display higher bias near the western bay, while the IPSL-CM6A-LR model exhibits higher bias over the southern regions. These findings highlight the performance variations among different climate models in reproducing Ocean Heat Content (OHC) in the Bay of Bengal. While some models demonstrate better agreement with observed data and exhibit lower bias, others show poorer performance and higher bias. The observed zero correlation and elevated p-values in the central region indicate that the models struggle to accurately capture OHC variability in this particular area.

There are a number of reasons why CMIP6 models may be having difficulty in the central Bay of Bengal:

- 1) The complex physical processes that control OHC in the central Bay of Bengal are not fully understood. OHC is influenced by a number of factors, including ocean currents, upwelling, and downwelling, as well as the exchange of heat between the ocean and the atmosphere. These processes are complex and can be difficult to simulate in climate models.
- 2) The central Bay of Bengal is a data-poor region. There is relatively little observational

261 data on OHC in the central Bay of Bengal. This makes it difficult to validate the performance  
262 of climate models in this region.

263 3) A coarse resolution climate model may not be able to adequately represent these small-  
264 scale features, which could lead to errors in its simulation of OHC in the central Bay of Bengal.

265 Understanding and quantifying these model uncertainties and biases are crucial for reliable  
266 climate projections and informed decision-making regarding the impacts of climate change in  
267 the Bay of Bengal region. Further research and model improvements are necessary to enhance  
268 the accuracy and reliability of climate models, particularly in capturing the complex dynamics  
269 and processes in the Bay of Bengal.

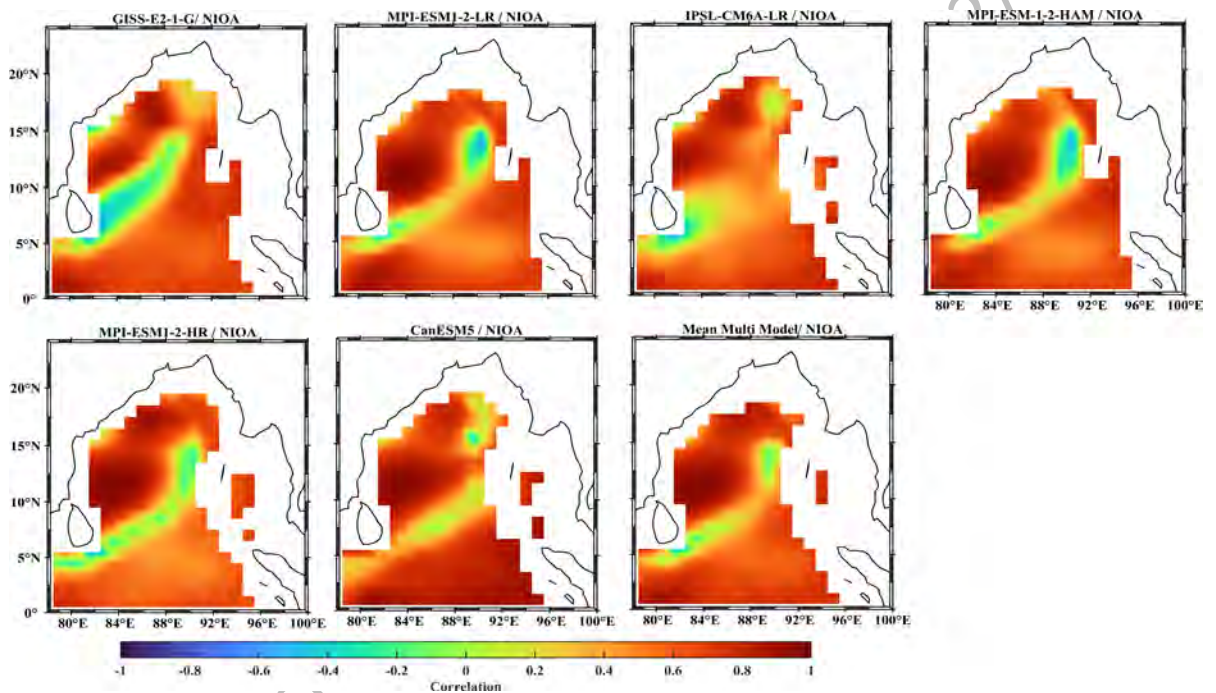


Figure 4.: Spatial Distribution of Correlation Coefficient.

#### 270 4.2. Monthly Climatology Variations of Ocean Heat Content

271 The key findings of the study are as follows:

272 1) The GISS-E2-1-G, MPI-ESM1-2-HR, and MPI-ESM-1-2HAM models show overall  
273 good performance in simulating OHC in the Bay of Bengal.

274 2) The mean multi-model of the CMIP6 models does not have a much better performance  
275 than the individual models.

276 3) The GISS-E2-1-G model shows that the Bay of Bengal is warmer from January to May

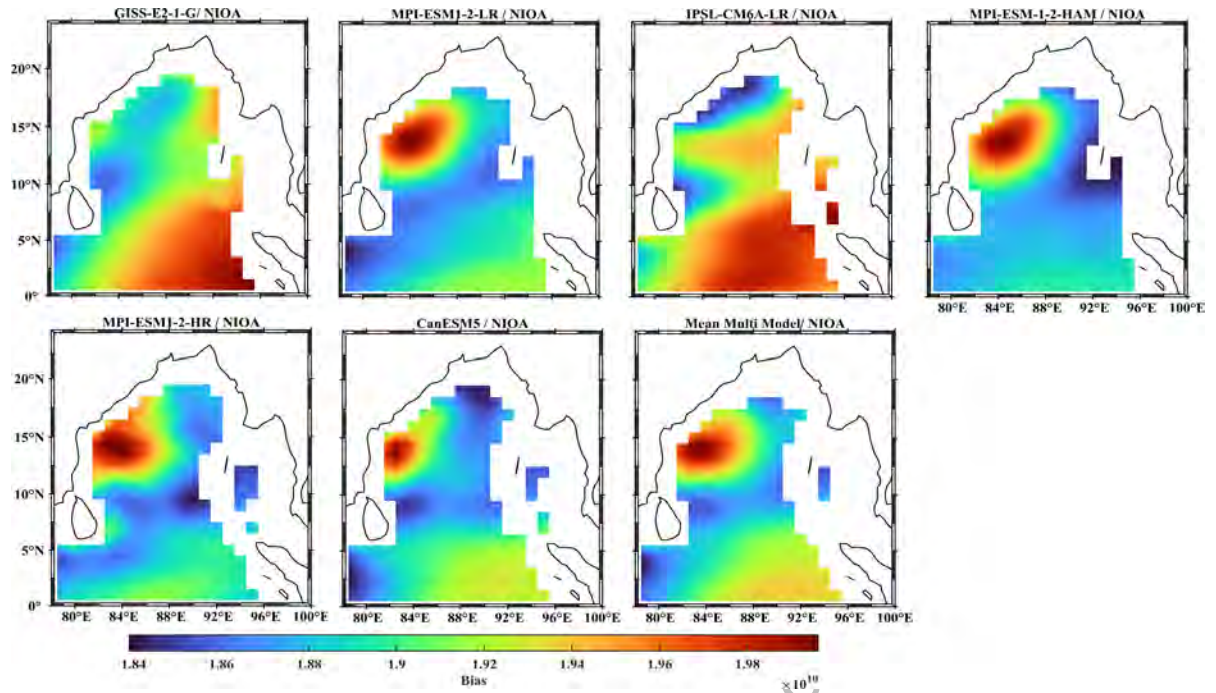


Figure 5.: Spatial Distribution of Bias.

and from July to October 6. The southern parts of the Bay of Bengal generally have less ocean heat content than the northern parts (Fig 6).

4) The monthly climatology of OHC data from the NIOA shows that the Bay of Bengal is warmer from February to May, and that the entire Bay of Bengal has high ocean heat content in June and July (Fig. 7).

Overall, the study found that the GISS-E2-1-G model is the best performing CMIP6 model for simulating OHC in the Bay of Bengal. The study also found that the Bay of Bengal is generally warmer in the northern parts than in the southern parts.

#### 4.3. Seasonal Climatology Variations of Ocean Heat Content

The seasonal climatology of GISS-E2-1-G is shown in figure 6. Monthly climatology variations of Ocean Heat Content (OHC) in the Bay of Bengal provide insights into the seasonal patterns of heat accumulation and distribution in this region of the Indian Ocean. The Bay of Bengal experiences unique climatic conditions influenced by monsoons, river runoff, and ocean currents, making it an important area to study OHC variations.

The OHC in the Bay of Bengal exhibits distinct monthly variations throughout the year figure 7. During the winter season (January of Figure 7), the northern region of the bay re-



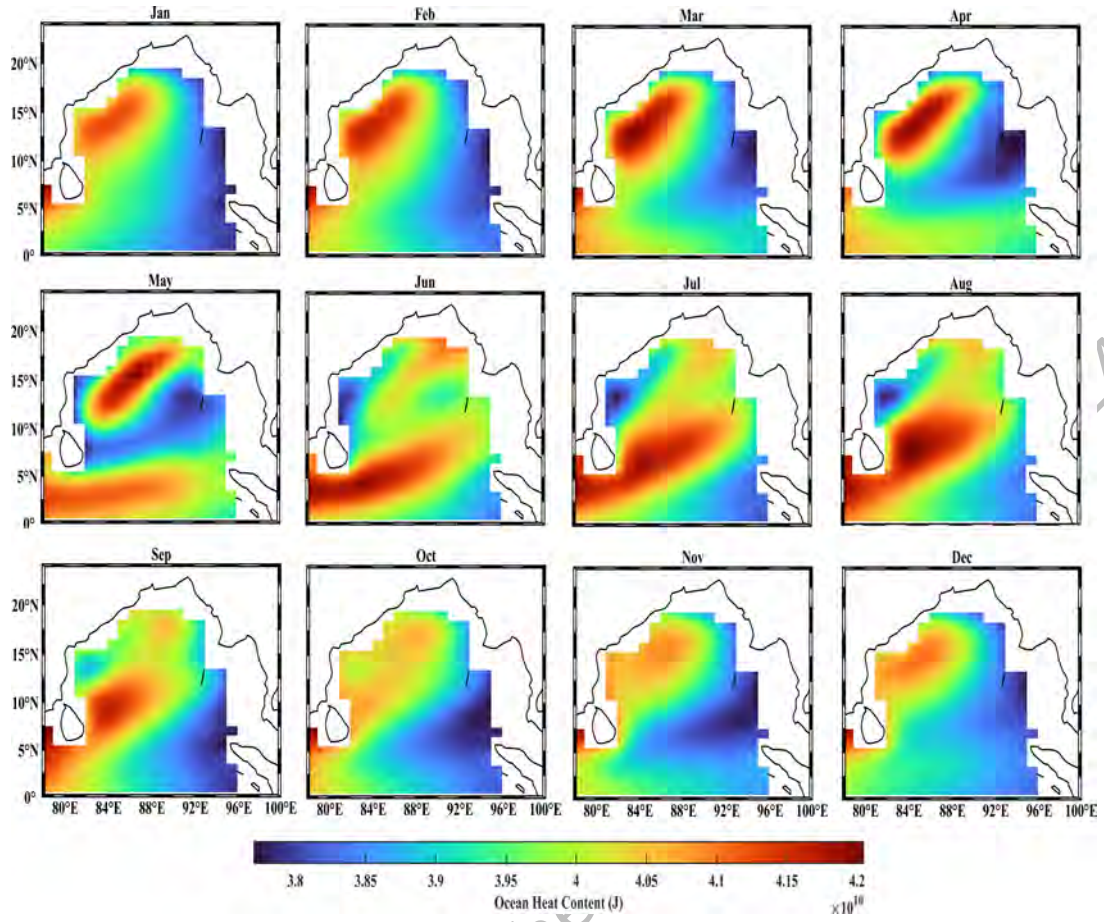


Figure 6.: Monthly Climatology Ocean Heat Content of GISS-E2-1-G

ceives cool and less saline water, leading to a decrease in OHC. The mid-Bay is in fact coolest in Nov-Jan, as can be seen in Figure 6. This leads to the flow of cool water southward, creating a surface layer of cooler temperatures. The freshwater inputs from rivers such as the Ganges, Brahmaputra, and Irrawaddy during the monsoon season (June-Sep) can create a less saline surface layer, affecting the stratification within the water column and increasing OHC. So, during the summer and consequently, monsoonal season, the bay experiences warmer temperatures as warm and saline waters from the northern Bay, influenced by the southwest monsoon, contribute to an increase in OHC. This can be seen as an increase (brown color) up to August.

#### 4.4. Annual Trends

Figure 8 presents the annual trends for all the models in relation to ocean heat content in the Bay of Bengal. The models MPI-ESM1-2-HR, MPI-ESM-1-2-HAM, and GISS-E2-1-G ex-

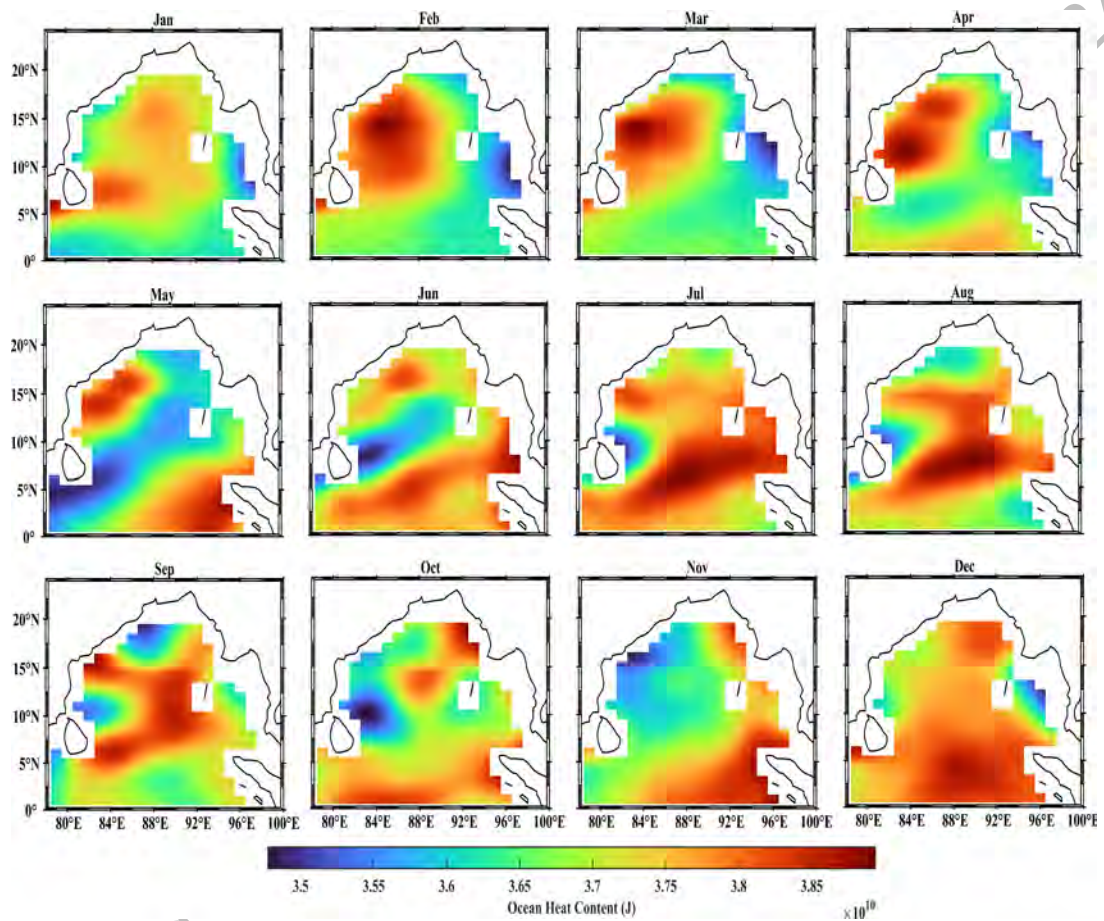


Figure 7.: Monthly Climatology Ocean Heat Content of NIOA data



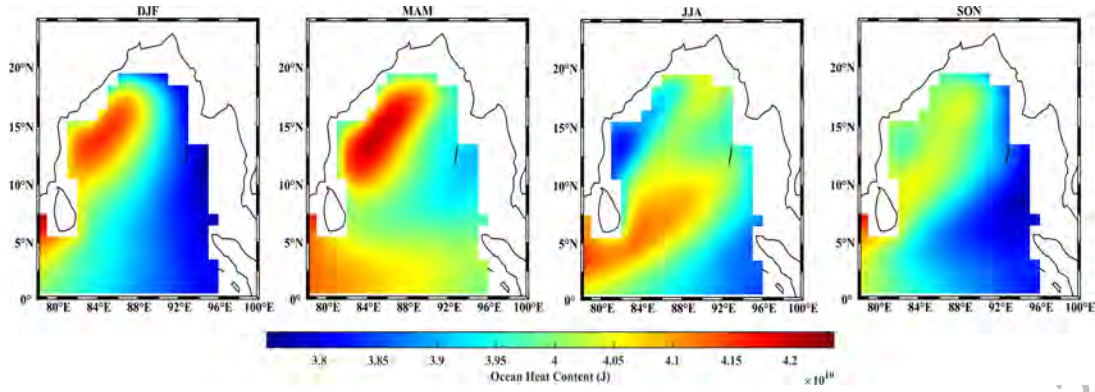


Figure 8.: Seasonal Climatology Ocean Heat Content GISS-E2-1-G

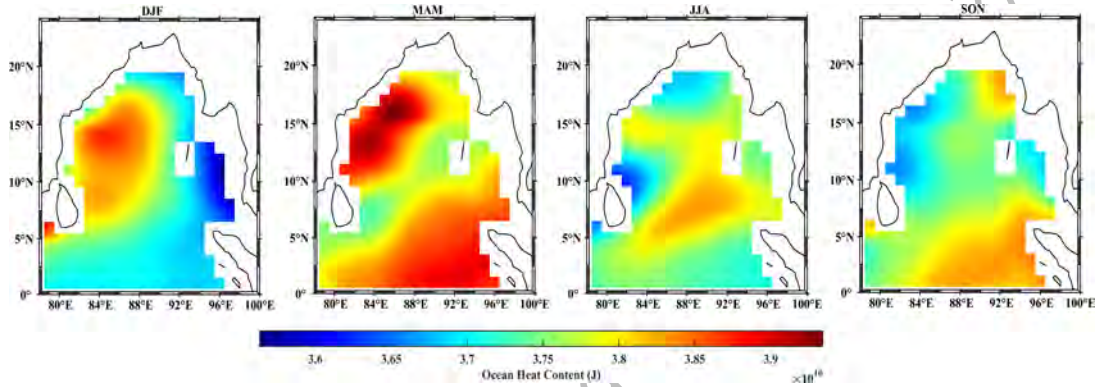


Figure 9.: Seasonal Climatology Ocean Heat Content of NIOA Data

hibit negative trends, indicating a decreasing pattern or a downward slope in the data over time. This suggests that there has been a net loss of heat from the ocean or a decrease in the accumulation of heat in the specified region. On the other hand, the remaining models display positive trends, indicating that heat is accumulating in the Bay of Bengal. It is not yet established which of these trends is accurate and continued monitoring, research, and modeling efforts are necessary to unravel the complex interactions between natural climate modes, monsoon dynamics, and anthropogenic influences, and their impacts on the heat content in the Bay of Bengal.

To further evaluate the performance of the models, time series graphs comparing the model values with the in-situ data from the RAMA Buoy at the location (15°N, 90°E) are shown in Figure 10. The data shown in Figure 10 clearly indicate that during the period 2007-2015, there is a noticeable decrease in OHC in the Bay of Bengal region, according to the best model GISS-E2-1G. This trend is due to the internal dynamics (variabilities) of that CMIP6 model. This trend could be due to influences in the inter-annual variations due to short-term changes

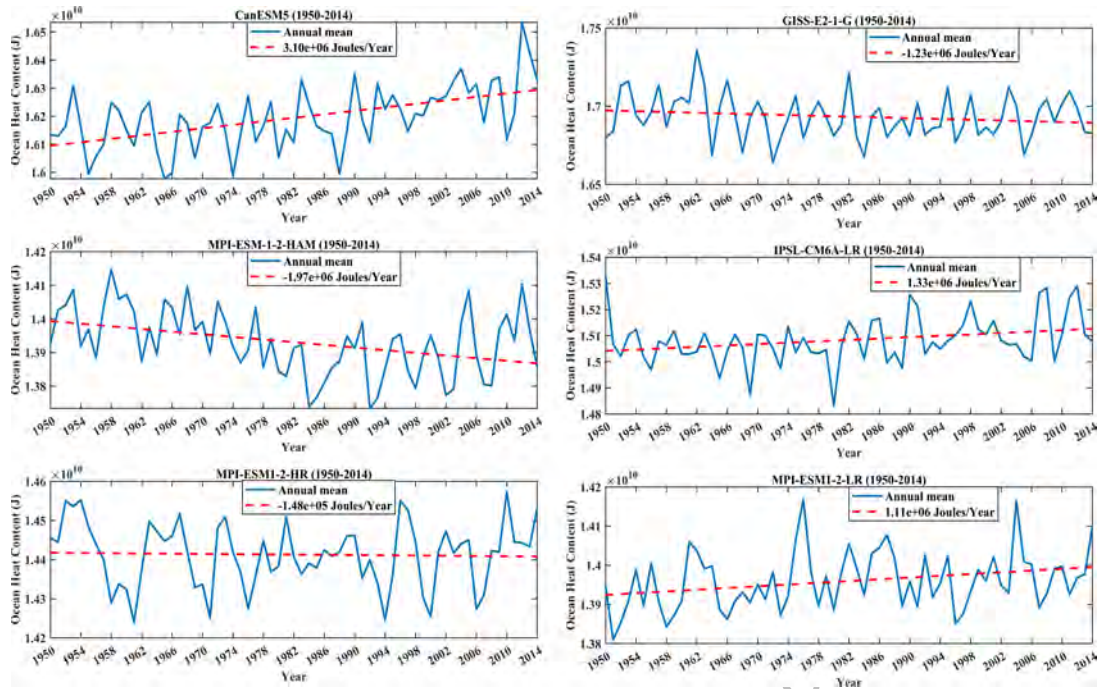


Figure 10.: Annual Trends for all models from 1950- 2014

in monsoon dynamics. The Indian summer monsoon,<sup>21</sup> which brings the majority of rainfall to the region, can undergo annual shifts in intensity and spatial distribution. These shifts can affect the heat content in the Bay of Bengal by altering the amount and timing of solar radiation, evaporation, changes in freshwater input,<sup>12</sup> and heat transfer due to circulation changes. Changes in monsoon patterns can result in periods of enhanced heat accumulation or reduced heat content in the region. The Fig 11 represents a multi-model mean for the same period. As can be seen there is a slightly upward trend in the graph. The OHC has been slowly increasing over the years. This is due to anthropogenic changes since the multi-model mean removes any internal variabilities of the CMIP6 models. Human-induced climate change may also play a role in the inter-decadal variation of OHC in the North Bay of Bengal.<sup>22</sup> Rising greenhouse gas concentrations and global warming can lead to long-term changes in sea surface temperatures, ocean currents, and atmospheric circulation patterns, influencing heat accumulation and distribution in the region. However, the specific impacts of climate change on inter-decadal variations are still being studied and are subject to ongoing research.

Throughout the years, the buoy data consistently show lower heat content compared to the models. This implies that the models tend to overestimate the heat content in the Bay of Bengal when compared to the actual observations from the RAMA Buoy. The higher values provided

336 by the models indicate an overestimation of the heat accumulation in the region.

337 These findings highlight the importance of considering observational data, such as the  
 338 RAMA Buoy measurements, for accurate assessments of ocean heat content. The lower heat  
 339 content experienced in the buoy data suggests that the models may have limitations or biases  
 340 in capturing the true heat content variability in the Bay of Bengal.

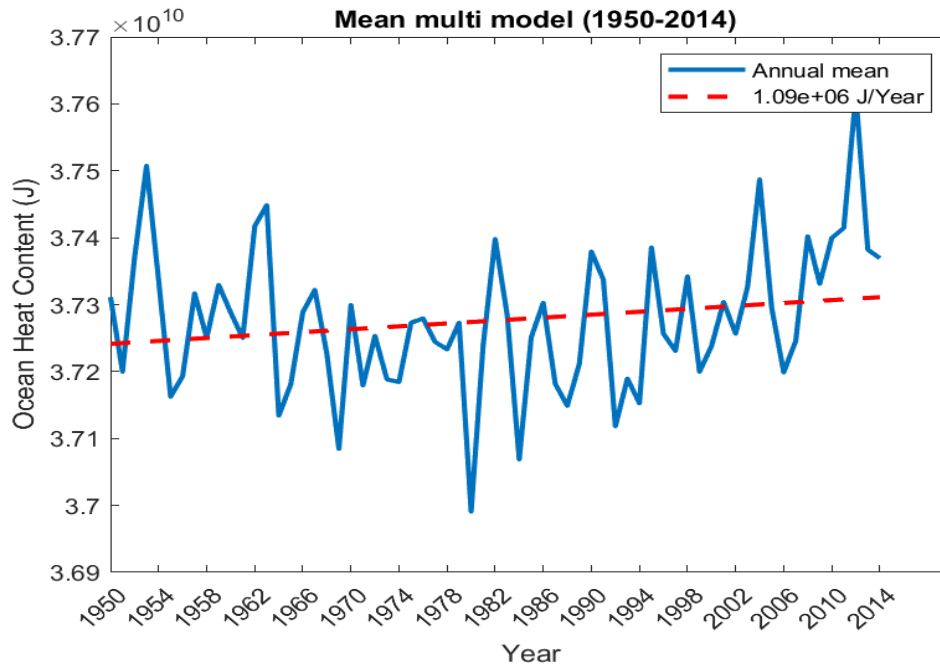


Figure 11.: Time series plots for OHC for multi-mean models from 2007- 2014

#### 341 4.5. Implications for the Indian Ocean Dipole

342 The interaction between the North and South Bay of Bengal, as observed in the CMIP6 mod-  
 343 els, has implications for the Indian Ocean Dipole (IOD). The IOD is a climate phenomenon  
 344 characterized by temperature gradients and atmospheric pressure differences between the east-  
 345 ern and western equatorial Indian Ocean. It exhibits positive and negative phases, with distinct  
 346 features for each phase.

347 In a positive IOD phase, the western Indian Ocean near the East African coast experiences  
 348 warm waters, accompanied by weaker easterly winds in the region. Conversely, during a neg-  
 349 ative IOD phase, the temperature gradient reverses, resulting in warm waters in the eastern  
 350 Indian Ocean, specifically near Indonesia and Australia.

351 Taking the specific year 2012 as an example, it was a negative phase of the IOD. During

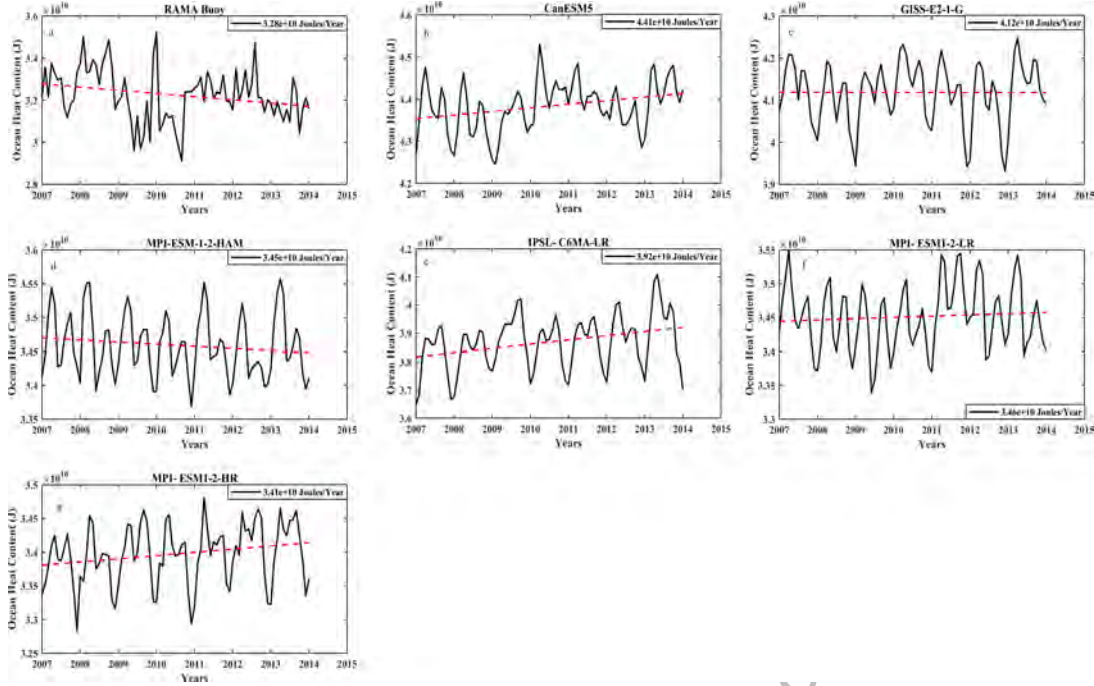


Figure 12.: Time series plots for OHC for all models from 2007- 2014 in comparison with in-situ data

this phase, the temperatures and subsequently the Ocean Heat Content (OHC) of the Bay of Bengal become higher than normal. This increase in OHC is evident in various datasets.<sup>23</sup> For instance, Figure 12a, which depicts data from the RAMA buoys, shows a spike in OHC between 2012 and 2013, indicating the impact of the negative IOD. Similarly, Figure 12c, representing the GISS model, also shows a notable rise in OHC during the same period. Fig 13 which details the GISS-E2-1G model for various months of 2012 depicts the same. The IOD was prominent from June-September in 2012. These observations highlight the agreement between the CMIP6 models and the climatic variations associated with the IOD, suggesting the potential utility of these models for climate predictions in the Bay of Bengal.

Overall, the interaction between the North and South Bay of Bengal and its influence on the IOD provide insights into the complex dynamics of the region and its potential implications for climate variability and prediction.

## 5. Conclusions

In this study, the performance of six CMIP6 models in capturing the variations of ocean heat content (OHC) in the Bay of Bengal was evaluated. The performance indices, includ-



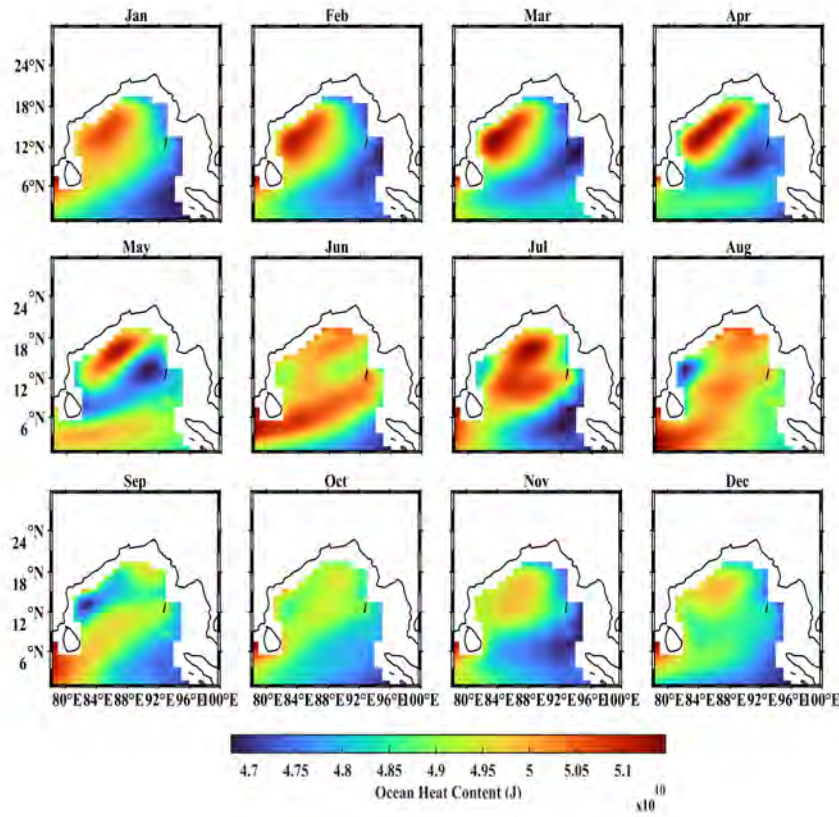


Figure 13.: Ocean Heat Content of GISS- E2-1-G in t-he year 2012 for a negative IOD year

ing RMSE, average error, absolute average error (AAE), and Willmott score, were used to assess the models' performance. All the 6 models were at confidence level of 95%. From Table 2 and 3, it is evident that the GISS-E2-1-G model exhibited the lowest RMSE ( $1.36 \times 10^{10}$ ), indicating better performance in capturing OHC compared to the other models. Conversely, the IPSL-CM6A-LR model had the highest RMSE ( $1.68 \times 10^{10}$ ), suggesting poorer performance. The negative average error across all models indicates that the predicted values consistently underestimated the actual values. The IPSL-CM6A-LR model also had the highest AAE ( $9.84 \times 10^9$ ), indicating poorer performance, while the GISS-E2-1-G model had the lowest AAE ( $6.13 \times 10^9$ ), indicating better performance. The Willmott score analysis further confirmed that the IPSL-CM6A-LR model exhibited poor performance (score of 0.64) compared to all other models, while the GISS-E2-1-G model demonstrated relatively better performance (score of 0.77) in the Bay of Bengal region. Overall, all models exhibited strong correlations in the vicinity of the bay and the southern part of the Bay of Bengal. However, a distinct spatial

380 pattern emerged, indicating zero correlation and p-values greater than 0.5 in the central region  
381 (Figure 4). This suggests that the models struggle to accurately capture OHC variability in this  
382 particular area.

383 Bias analysis revealed that all models demonstrated positive bias, indicating an overesti-  
384 mation of the reference datasets. Furthermore, different models exhibited varying levels of  
385 bias in different regions of the Bay of Bengal. The models MPI-ESM1-2-LR, MPI-ESM-1-  
386 2HAM, MPI-ESM1-2-HR, and CanESM5 displayed higher bias near the western bay, while  
387 the IPSL-CM6A-LR model exhibited higher bias over the southern regions. These variations  
388 in bias highlight the performance differences among the different climate models in reproduc-  
389 ing OHC in the Bay of Bengal. To analyze the monthly climatology variations of OHC, data  
390 spanning 65 years were utilized. The Bay of Bengal experiences unique climatic conditions  
391 influenced by monsoons, river runoff, and ocean currents, making it a crucial area to study  
392 OHC variations. During the summer season (March-May), there was a noticeable increase in  
393 temperature and consequently, OHC in the Bay of Bengal region, as indicated by the NIOA  
394 Data in Figure 8. This might be due to a combination of heat flux, flux of warm saline waters  
395 or other aspects of circulation, which warrants further study.

396 The annual trends in OHC for the CMIP6 models showed both positive and negative pat-  
397 terns (Figure 9). The models MPI-ESM1-2-HR, MPI-ESM-1-2-HAM, and GISS-E2-1-G ex-  
398 hibited negative trends, suggesting a net loss of heat from the ocean or a decrease in heat  
399 accumulation. CMIP6 models each have a different internal variability that makes it diffi-  
400 cult to compare with the observations (CMIP models have different internal variability. This  
401 means that different models will simulate different amounts of variability in the climate sys-  
402 tem, even if they are forced with the same external forcing). But our aim, was to find the  
403 CMIP6 model that can predict the internal variability of Bay of Bengal. We are trying to find  
404 the model that has the internal variability to study the phenomena of Bay of Bengal. This in-  
405 ternal variability can also be the IOD. So our conclusion is that GISS-E2-1G is probably the  
406 most suitable CMIP6 model to study IOD/any other internal variability in the Bay of Ben-  
407 gal. Conversely, the remaining models displayed positive trends, indicating an accumulation  
408 of heat in the Bay of Bengal. The comparison of model values with the RAMA Buoy data  
409 at the location (15°N, 90°E) provided valuable insights. The buoy data consistently showed  
410 lower heat content compared to the models, indicating an overestimation of heat accumulation  
411 by the models. This emphasizes the importance of incorporating observational data, such as  
412 the RAMA Buoy measurements, to improve the accuracy of OHC assessments in the Bay of

Bengal.

In conclusion, the evaluation of CMIP6 models for OHC in the Bay of Bengal revealed variations in performance among the models. The GISS-E2-1-G model demonstrated better performance, while the IPSL-CM6A-LR model exhibited poorer performance. It was also seen that the CMIP6 models follow the buoy trend of higher OHC during a negative IOD year (with an example taken as 2012). But it must be noted that understanding and quantifying these model uncertainties and biases is crucial for reliable climate projections and informed decision-making in the Bay of Bengal region. Further research and model improvements are necessary to enhance the accuracy and reliability of climate models, particularly in capturing the complex dynamics and processes specific to the Bay of Bengal.

## References

1. Trenberth KE, Fasullo JT, Kiehl J. Earth's global energy budget. *Bulletin of the American Meteorological Society*. 2009;90(3):311-323.
2. Meyssignac B, Boyer T, Zhao Z, *et al.* Measuring Global Ocean Heat Content to Estimate the Earth Energy Imbalance. *Frontiers in Marine Science*. 2019;6.
3. M. Stocker T, D. Qin GKP, Tignor M, *et al.* Contribution of Working Group I to the Fifth Assessment Report of the Intergovernmental Panel on Climate Change. *Cambridge University Press, Cambridge, United Kingdom and New York, NY, USA*. 2013:1535pp.
4. Taylor K, Stouffer R, Meehl G. An overview of CMIP5 and the experiment design.. *Bulletin of the American Meteorological Society*. 2012;93(4):485-498.
5. Eyring V, Bony S, Meehl, *et al.* Overview of the Coupled Model Intercomparison Project Phase 6 (CMIP6) experimental design and organization.. *Geoscientific Model Development*. 2016;9(5):1937–1958.
6. Meehl GA, Senior CA, Eyring V, *et al.* Context for interpreting equilibrium climate sensitivity and transient climate response from the CMIP6 Earth System Models.. *Science Advances*. 2020;6(26):1-10.
7. Vivekanandan E, Hermes R, Satpathy S, Ravindranath P, Balachandran . Climate change effects in the Bay of Bengal Large Marine Ecosystem. In *Frontline Observations on Climate Change and Sustainability of Large Marine Ecosystems. United Nations Development Programme (UNDP)*. 2012:97-111.
8. Vinayachandran PN, Matthews AJ, Vijay Kumar K, *et al.* BoBBLE (Bay of Bengal Boundary Layer Experiment): Ocean-atmosphere interaction and its impact

- on the South Asian monsoon.. *Bulletin of the American Meteorological Society*. 2013;94(8):1257-1276.
9. Albert J, Bhaskaran PK. Ocean heat content and its role in tropical cyclogenesis for the Bay of Bengal basin. *Climate Dynamics*. 2020;55:3343-3362.
  10. Shetye SR, Gouveia AD, Shankar D, *et al*. Hydrography and circulation of the western Bay of Bengal during the northeast monsoon.. *Journal of Geophysical Research: Oceans*. 15 June 1996;Volume101, IssueC6:14011-14025.
  11. Sengupta D, Bharath Raj GN, Shenoi SSC, Ravichandran M. Surface freshwater from the Bay of Bengal runoff and Indonesian throughflow in the tropical Indian Ocean.. *Geophysical Research Letters*. 2016;43(11):5964-5972.
  12. Sumangala D, Joshi A, Warrior H. Modelling freshwater plume in the Bay of Bengal with artificial neural networks. *Current Science*. 2022;123 (1):73.
  13. Lyman JM, Johnson GC, Purkey SG. Robust warming of the global upper ocean. *Nature Climate Change*. 2021;11(8):664-671.
  14. Durack PJ, Gleckler PJ, Landerer FW, Taylor KE. Quantifying underestimates of long-term upper-ocean warming. *Nature Climate Change*. 2014;4(11):999-1005.
  15. Palmer MD, Good SA, Kennedy JJ, Berry DI, Dunn RJ, Haines K. A comprehensive uncertainty assessment of global satellite-based estimates of ocean heat content.. *Journal of Geophysical Research: Oceans*.. 2021;126(2):e2020JC016957.
  16. Kumar V, Joshi AP, Warrior HV. Assesment of the CMIP6 models to study interseasonal SSTvariabilities in the BoB. *ISH Journal of Hydraulic Engineering*. 2022.
  17. Bhattacharya B, Mohanty S, Singh C. Assessment of the potential of CMIP6 models in simulating the sea surface temperature variability over the tropical Indian Ocean. *Theoretical and Applied Climatology*. 2022;148:585-602.
  18. LI J, SU J. Comparison of Indian Ocean warming simulated by CMIP5 and CMIP6 models. *Atmospheric and Oceanic Science Letters*. 2020;13:604-611.
  19. Willmott CJ, Robeson SM, Matsuura K. A refined index of model performance. *International Journal of Climatology*. 2012;32:2088-2094.
  20. Joshi AP, Chowdhury RR, Kumar V, Warrior HV. Configuration and skill assessment of the coupled biogeochemical model for the carbonate system in the Bay of Bengal. *Marine Chemistry*. 2020;226.
  21. Simpson M, Warrior H, Raman S, Aswathanarayana P, Mohanty U. Sea-breeze-initiated rainfall over the east coast of India during the Indian southwest monsoon. *Natural Hazards*. 20-7;42:401-413.
  22. Nath S, KOTAL SD, Kundu PK. Decadal variation of ocean heat content and



- 482 tropical cyclone activity over the Bay of Bengal. *Journal of Earth System Science*.  
483 Feb 2016;125(1):73.
- 484 23. Han W, McCreary JP, Anderson DL. Dynamics of intraseasonal sea surface tem-  
485 perature variability in the Bay of Bengal.. *Journal of Climate*. 2017;30(9):3095-  
486 3114.

Unedited version published online on 20/02/2024